ELSEVIER

Journal of Molecular Catalysis A: Chemical 119 (1997) 57–67

JOURNAL OF MOLECULAR CATALYSIS A: CHEMICAL

Supported oxide overlayers: A link between macroscopic and microscopic properties

Furio Corà *, C. Richard A. Catlow

Davy Faraday Research Laboratory, The Royal Institution of Great Britain, 21 Albemarle Street, London W1X 4BS, UK

Received 6 June 1996; accepted 9 July 1996

Abstract

In this paper we examine supported oxide overlayer catalysts. We first show that, despite the possible combinations of support and overlayer employed, the whole class shows several chemical and structural analogies and can be treated as a uniform group. Based on the trends highlighted, we propose two different geometries of the interface, that we have labelled *mechanical mixing* and *chemical deposition* models. We further derive a set of equations that link the relevant experimental variables (overlayer loading, support face exposed, overlayer face exposed, oxidation state and local coordination number of the overlayer cation) with one another and to energy parameters obtained at the microscopic level. We show that the support modifies the reducibility of the overlayer cation and can even force a different stoichiometry in the overlayer, as suggested by the stability of our chemical deposition model at low loadings, thus influencing the catalytic behaviour of the supported phase.

Keywords: Computer modelling; Interfaces; Supported oxides; Oxide films; Surface structure; Catalysis

1. Introduction: The use of supported overlayers in catalysis

Supported transition metal oxides represent a class of heterogeneous catalysts that have recently found application in a variety of technologically important reactions: examples include the selective catalytic reduction (SCR) of nitrogen oxides with ammonia [1–12], oxidation of alkanes [2,13–15], decomposition of alcohols [2,16–18], reduction of aromatic nitroderivatives to anilines [18], isomerisation [16,18] and polymerisation [19] of alkenes and partial oxidation of alcohols to aldehydes [20,21]. Oxides of the first half of the transition series (V_2O_5, CrO_3, Nb_2O_5, MoO_3, WO_3, Re_2O_7, with the addition of CuO) are the most widely used overlayers; other high valence oxides (TiO_2, SiO_2, ZrO_2, Al_2O_3) and isostructural fluorides (MgF_2) are used as supports.

With respect to standard methods of activating solids via doping in the bulk, supported overlayers have several advantages: the high concentration of active sites on the surface; an easier control of the preparation process, that eliminates the variable represented by the concentration profile of the dopant

* Corresponding author. E-mail: furio@ri.ac.uk.

PII S1381-1169(96)00469-4

as a function of its depth in the support; the increased possibility of fine-tuning the properties of the exposed surface by appropriate modifications of only one of the two components. In this way we can maximise the selectivity or the yield (or both) [22] of the catalytic process, or the stability of the catalyst under reaction conditions.

Despite the increasing number of applications, very little is known of the basic factors governing the structure and properties of supported overlayers; due to the inherent difficulty in characterizing the interface, detailed structural models are not always available and knowledge of the active state of the surface is still lacking. The supported material can show properties that are entirely different from those of the unsupported system, most notably in its surface structure [22–24]. Understanding the role of the support is therefore of crucial importance: attempts have been made to correlate ease of formation and thermal stability with the ratio of charges and ionic radii [25] or to the difference of acid/basic properties between support and overlayer [26,27]; the increased activity of the binary system has been attributed to an increased redox ability of the overlayer [28–30] or to an increased acidic strength of supported surface sites [26,27,31] but an exhaustive theory that is able to rationalise the data and predict the behaviour of these systems is still lacking.

This paper aims to advance our understanding of the support/overlayer interaction. We show that, despite the number of possible combinations of support and overlayer, the whole class of materials shows a number of common features, allowing them to be represented as a uniform group. We proceed by first identifying trends in the experimental literature (Section 2) and then proposing two geometrical models of the interface system (Section 3). The energy parameters obtained from a microscopic description can be used to derive the relative stabilities of the different structures at the macroscopic level; the shape of the oxide particle deposited and its ability to 'spread' over the support are shown to depend on the same parameters. Section 4 contains general comments and conclusions arising from the models presented.

2. Analogies in active oxide overlayer catalysts

Useful trends can be noted in the active components of supported oxide overlayers, relating to the chemical and structural properties of the constituents.

2.1. Chemical analogies

If we mark on the periodic table the elements whose oxides have been used in either a support or overlayer, as shown in Fig. 1, a number of observations become evident:

- Elements employed occupy the entire first half of the d-block, plus copper, aluminium and silicon. The oxides of all the elements highlighted are characterized by amphoteric properties; the balance between acid and basic behaviour is strongly influenced by the environment and it is reasonable to assume that this influence is very pronounced in the neighbourhood of the interface.
- Cations are always reported as being in their highest possible oxidation state. For each element this oxidation state is associated with the highest acidic character; we can therefore hypothesize a role of the surface acidity in the catalytic activity, in agreement with references [26,27,31]. Surface acidity can play an important role, indeed, in the adsorption of basic reactants as employed in most catalytic processes (for instance the ammonia and NO molecules of the SCR).
- All the elements highlighted, with the exceptions of aluminum and silicon, can exist in several oxidation states. The ease of undergoing redox reactions is generally higher for elements employed

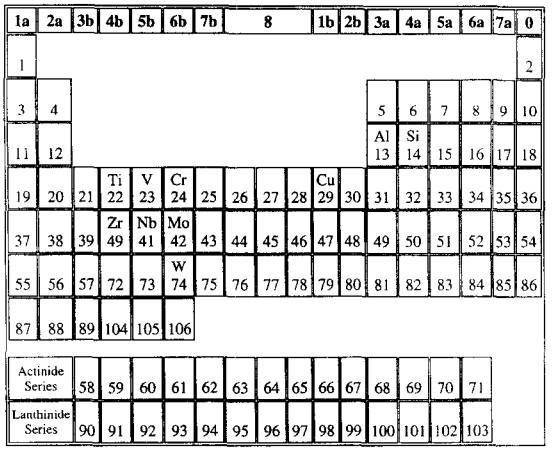

Fig. 1. Disposition of the components of active overlayer catalysts in the periodic table.

in the overlayer than in the support. This property of the overlayer can be linked with other experimental evidence: the correlation between activity and reducibility of the surface [28,29] and between the concentration of reduced surface species and reaction rate [30,32].

- The factors of acidity and redox properties are probably both important. If we assume a reaction mechanism in which adsorption of basic reactants (A) on the surface (Eq. (1)) and the electron transfer from a reduced surface atom to the admolecule (Eq. (2)) represent two elementary steps, the central role is the acid strength of the surface if Eq. (1) is the rate-determining step; while the surface redox properties would be the most important factors if the rate-determining step is Eq. (2).

$$M_s + A_{1(g)} \rightleftharpoons (M{:}A_1)_s \tag{1}$$

$$(M{:}e^-)_s + A_2 \rightleftharpoons (M{:}A_2^-)_s \tag{2}$$

The same catalytic system can show either behaviour depending on experimental variables, like concentration of reactants, flux velocity and temperature.

- There are also general chemical relationships on comparing the overlayer with its support; in particular the formal oxidation state of the supported metal is always higher than that of the supporting element. This observation can be re-expressed in a different way, regarding the stoichiometry: in the system $M'O_x/M''O_y$, the supported overlayer is always richer in oxygen than the support ($x > y$) The only exception occurs with copper oxides. The two formulations are equivalent for binary oxides, but would have different implications when considering an extension to ternary systems. In the interface $M'O_x/M''M'''O_y$, for instance, we would generally have different results depending on whether we compare oxygen/metal ratios (x/y) or the individual oxidation states of M′, M″ and M‴. Unfortunately no experimental result is reported in the literature for systems with these characteristics to validate either hypothesis; it seems likely, however, that the stoichiometry requirement (the O/M ratio) would prevail in the latter case.

This comparison seems therefore to suggest that catalytically active overlayers can be obtained combining two amphoteric components: one (the support) with fixed oxidation state and the other (overlayer) with an oxidation state that is more easily variable and greater than the support. The overall system must display acidic surface sites.

2.2. Structural analogies

The structural properties of the oxides employed are less homogeneous than their chemical properties. Table 1 lists the stable crystalline structures of the pure components, as reported in Ref. [33]: they range from rock-salt to layered, from one-dimensional chains to perovskite-like and have apparently very little in common. To find some common feature we must move from the overall crystal to the local structure around single cations. Coordination numbers and metal–oxygen bond distances are also reported in Table 1.

- In the oxides used as overlayer, with the exception of CuO and CrO_3, cations are surrounded by distorted oxygen octahedra; the average cation–metal bond length is also similar, ranging from 1.90 to 2.02 Å. In CuO, where the local structure around Cu is reported as being square planar, two additional oxygens are present, at a higher distance and in a direction perpendicular to the plane, to complete the octahedron. The stable CrO_3 polymorph is characterised by linear chains of tetrahedrally coordinated cations; nonetheless, chromium in lower oxidation states adopts octahedral coordination.
- The oxides used as supports show greater variability. In MgO, Al_2O_3 and the two polymorphs of TiO_2 there is octahedral coordination, but in zirconia the cation has coordination 8 and 7 and Si is, of course, tetrahedrally coordinated in silica. For the first group, the structural and chemical analogy suggests an easy interchange of cations with the overlayer; to understand the consequence of the different structure of silica and zirconia we must develop models for the support–overlayer interaction, which is done in the next section.

A final comment is needed, concerning catalyst preparation. Although different methods have been attempted (see for instance Ref. [2]), that generally employed consists of a chemical deposition of the overlayer on the support, from salts of the overlayer element. We can therefore assume that the starting structure of the support, both its phase and also the faces exposed, are defined; this is a factor of primary importance. No assumption can however be made regarding the overlayer oxide: the examination of its preferred structures when pure and in bulk can serve as a guideline in studying its

Table 1
Crystal structure and local disposition of oxygens around the cation for active overlayer oxides. Oxides are reported in order of increasing oxidation state of the cation. The symbol N represents the coordination number of the cation; $\langle r \rangle$ the average distance (in Å) between the cation and its N nearest oxygens. Individual metal–oxygen distances are indicated as r_i in increasing order. MgF_2 has been added for comparison with TiO_2

Oxide	Space group	Structure	N	$\langle r \rangle$	r_1	r_2	r_3	$r4$	r_5	r_6	r_7
MgO	Pm3m	rock-salt	6	2.11	2.11	2.11	2.11	2.11	2.11	2.11	
CuO	C2/c	monoclinic	4 (6)	2.22	1.95	1.95	1.95	1.95	2.77	2.77	
A_2O_3	R-3c	corundum	6	1.92	1.86	1.86	1.86	1.97	1.97	1.97	
SiO_2	$P3_12$	quartz	4	1.61	1.61	1.61	1.61	1.61			
MgF_2	P4/mnm	cassiterite	6	1.99	1.98	1.98	2.00	2.00	2.00	2.00	
TiO_2	P4/mnm	rutile	6	1.92	1.91	1.91	1.91	1.91	1.94	1.94	
TiO_2	I4/amd	anatase	6	1.94	1.93	1.93	1.93	1.93	1.97	1.97	
ZrO_2	Fm3m	fluorite (cubic)	8	2.20	2.20	2.20	2.20	2.20	2.20	2.20	2.20
ZrO_2	$P2_1/c$	tetrag. zirconia	7	2.16	2.05	2.06	2.15	2.16	2.19	2.22	2.28
V_2O_5	Pmmn	layered	6	1.99	1.54	1.77	1.88	1.88	2.03	2.83	
Nb_2O_5	I4/mmm		6	2.02	1.63	1.63	1.97	1.97	2.45	2.45	
CrO_3	Ama	1-D chains	4	1.80	1.79	1.79	1.81	1.81			
MoO_3	Pbnm	layered	6	2.00	1.68	1.68	2.03	2.03	2.30	2.31	
WO_3	P4/nmm	perovskite-like	6	1.90	1.64	1.86	1.86	1.86	1.86	2.30	

structure when supported, but should in no way limit the range of geometries considered. An exception is represented by the preparation route that involves mixing the gels of the two components; in this case the overlayer cation interacts with the support before the structure of the latter is set, and it can therefore influence the final crystalline habit of the whole system. In the following section we limit our consideration to the first case and assume the support structure is known and fixed.

3. Two geometrical models for the interfaces

Let us consider two compounds that satisfy all the chemical conditions outlined in Section 2.1. For simplicity, we take two oxides with octahedral coordination, and stoichiometry $M'O_x$ and $M''O_y$ (with $x > y$). Fig. 2 reports two such structures: they represent a two-dimensional projection of anatase (TiO_2) and tungsten trioxide (WO_3) along the $\langle 001 \rangle$ direction. Following from Section 2.1, let $M''O_y$ be the support and $M'O_x$ the overlayer.

We refer to a simplified, macroscopic, description of the interface, where we assume that the particle of M′-based compound deposited on the support has a cylindrical shape of radius r and height h, as shown in Fig. 3. Both r and h are discrete variables, in particular h is related to the number of M′ overlayers deposited; at a macroscopic level they can be treated as continuous. Following the

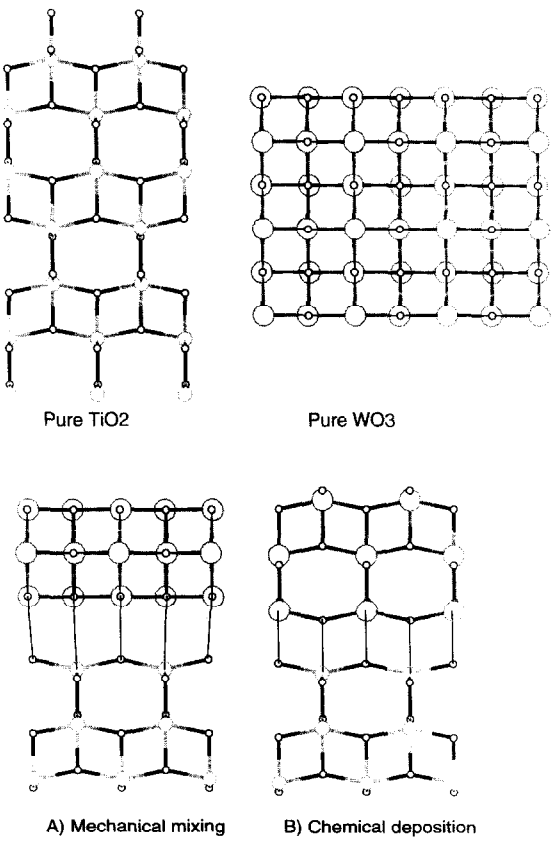

Fig. 2. Structure of pure oxides $M''O_y$, and $M'O_x$ (upper plots) and the two proposed structures for the interface (bottom plots). Small circles represent the oxygen ions; larger circles the metal cations.

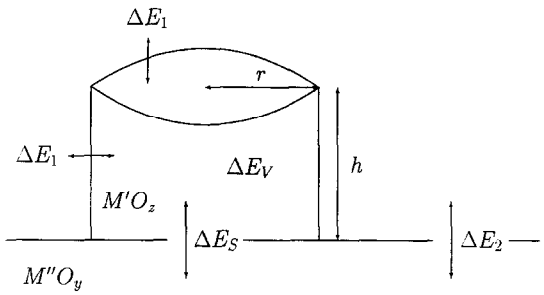

Fig. 3. Cylindrical particle of $M'O_z$ deposited on the $M''O_y$ support. The geometric parameters employed and the contributions to the total energy of the interface system, as defined in the text, are highlighted in the picture.

discussion in Section 2.2, we consider the structure of the $M''O_y$ sub-system as fixed, while we do not impose any constraint to the stoichiometry and to the structure of the M′ oxide and indicate the generic overlayer as $M'O_z$.

For subsequent reference, we divide the formation of the interface system into two elementary steps: a solid-state reaction that describes the phase transition of the M′ oxide from its structure when pure ($M'O_x$) to its structure when supported ($M'O_z$) and the subsequent deposition of $M'O_z$ on the support:

$$\text{pure } M'O_x \rightarrow \text{pure } M'O_z + \frac{x-z}{2} \cdot O_{2,(g)} \tag{3}$$

$$\text{pure } M'O_z \rightarrow \text{supported } M'O_z \tag{4}$$

The energy of the interface system with respect to the separate pure components can be divided into surface (ΔE_S) and volume (ΔE_V) contributions:

$$\Delta E = \sum_i s_i \cdot \Delta E_{S(i)} + v \cdot \Delta E_V \tag{5}$$

The sum extends to all surfaces present (i); s_i and v represent the area of the ith surface and the volume of the $M'O_z$ particle, respectively. The volume energy ΔE_V is defined as the difference energy per unit volume of $M'O_z$ accompanying Eq. (3).

We finally assume, at least to a first approximation, that all the energy values involved are purely geometric parameters of the system, and do not depend on the quantity of M′ deposited.

Referring to the geometry shown in Fig. 3, the total energy of the system is given by:

$$\Delta E = \pi r^2 h \cdot \Delta E_V + \pi r^2 \cdot \Delta E_S + (2\pi rh + \pi r^2) \cdot \Delta E_1 - \pi r^2 \cdot \Delta E_2 \tag{6}$$

where ΔE_1 and ΔE_2 are the surface energies of $M'O_z$ and $M''O_y$, respectively, and ΔE_S the interface energy. The last term takes into account that in the creation of the interface, part of the support surface has been covered by the overlayer and its contribution must be subtracted from the total energy.At a given quantity of M′ deposited on the support, c, the shape of the M′ particle is obtained by minimising the quantity ΔE (Eq. (6)), subject to the constraint:

$\pi r^2 h = cv_o$, c = constant

v_o is the volume per formula unit of $M'O_z$. Substituting in Eq. (6) and differentiating, we obtain:

$$r_o(c) = \left\{ \frac{c \cdot v_o \cdot \Delta E_1}{\pi \cdot (\Delta E_S + \Delta E_1 - \Delta E_2} \right\}^{1/3} \tag{7}$$

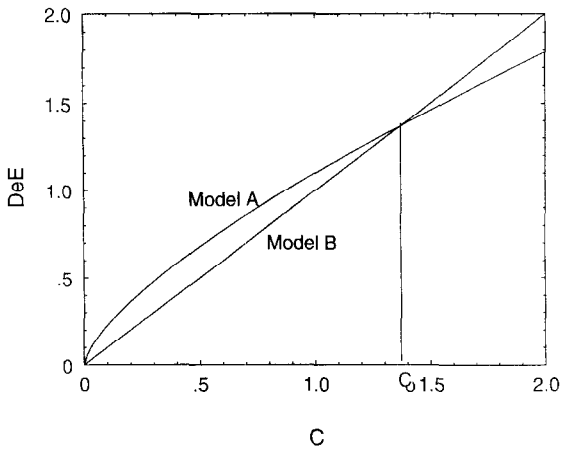

Fig. 4. Total energy (E) of the interface system as a function of the volume of overlayer deposited (c) according to models A and B presented in the text. The surface energy contribution, ΔE_S prevails in model A, the volume contribution, ΔE_V in model B; at low loadings the high ratio between surface area and volume favours the second structure.

Eq. (7) gives the shape of the cylindrical $M'O_z$ particle that minimizes the total energy; it is a function of all the surface energies involved, but does not depend on the volume energy. Replacing $r_0(c)$ in Eq. (6), we obtain the total energy of the system as a function of c:

$$\Delta E(c) = cp \cdot v_o \cdot \Delta E_V + 3\pi^{1/3} c^{2/3} \cdot v_o^{2/3} \Delta E_1^{2/3} \cdot (\Delta E_S + \Delta E_1 - \Delta E_2)^{1/3} \tag{8}$$

We identify a volume contribution, proportional to the amount of M′ deposited, c, and a surface energy proportional to $c^{2/3}$.

It is important to note that so far we made no assumption as to the structure of the interface and the set of Eqs. (7) and (8) is therefore of general applicability.

We now proceed a step further and formulate a microscopic geometry of the interface $M'O_x/M''O_y$, in the light of the similarities outlined in Section 2. We apply Eqs. (7) and (8) to two microscopic geometries, that correspond to extreme chemico–structural descriptions of the interface: in the first (A) each component retains its native structure, while in the second (B) we force the overlayer to assume the same structure of the support, in such a way as to give a perfect epitaxial match. The bottom part of Fig. 2 shows schematically the two possibilities. In case A, the effect of ΔE_V is minimised compared to ΔE_S; vice-versa, in case B the structure is continuous through the interface and we minimise the effect of ΔE_S (Fig. 4).

Some detailed application of model A can be found in the recent literature [34,35]. Those studies assume that the binary system retains its long-range periodicity; the interface is obtained by a matching of the lattice parameters (a, b) of the two surfaces exposed:

$$\begin{cases} m'a' \simeq m''a'' \\ n'b' \simeq n''b'' \end{cases} \tag{9}$$

Small mismatches can be accommodated by the overlayer; this introduces lateral strains in the interface and the distortion can activate the catalytic behaviour of the supported compound. This concept has been applied to the MgO/Mo system [35]; the activity of supported MgO towards the dissociation of water molecules has there been correlated to the increase in the lattice parameter of supported with respect to pure MgO. The change was forced by the mismatch between MgO (overlayer) and Mo (support). Similarly, Sayle et al. [34] found that the structure of the V_2O_5

monolayer on an anatase substrate is substantially distorted, leading to changes in the catalytic behaviour. These studies show that the chemical activation of the overlayer is possible following this procedure.

Applying Eqs. (7) and (8) to the interface geometry of model A, we note that the supported component has the same structure as in pure $M'O_x$, and ΔE_V^A, is negligible. A new volume contribution $\Delta E_V''$ must however be introduced, to account for the stretching of the supported $M'O_x$ particle caused by its matching the lattice parameters of the support. Since this contribution involves only a relaxation and not a reconstruction of the M′ oxide, it is reasonable to assume that $\Delta E_V''$ is lower than the value ΔE_V of Eq. (3). The most important contribution to $\Delta E^A(c)$ is therefore due to the surfaces.

The shape of the cylindrical particle depends on the ratio between surface energies, and $r_o(c)$ increases when increasing ΔE_1 compared to ΔE_2 and ΔE_S. In this case the overlayer will be 'spread' over the support. Vice versa, if ΔE_1 is small compared to ΔE_S, the chemical deposition of $M'O_x$ on $M''O_y$ is not favoured and the dimension of the contact area tends to zero; this can be interpreted on a microscopic scale as a tendency of the two sub-systems to separate.

Model B has not been described in the literature for oxide/oxide interfaces, to date. In the geometry examined, both components of the interface have the same structure and lateral strains are negligible, but a vertical strain is introduced in the overlayer by forcing M′ to have a structure that is different from its own. In this way we transfer the interface strain from the oxygen sub-lattice to the metal cations.

The stoichiometry of the overlayer is now $M'O_y$, and Eq. (3) can be expressed as:

$$\begin{cases} 2\,O_{(s)}^{2-} & \rightleftharpoons O_{2,(g)} + 4\,e_{(s)}^- \\ 4\,e_{(s)}^- + 2(x-y)\cdot M'O_x & \rightleftharpoons 2(x-y)\cdot M'O_y \end{cases} \tag{10}$$

where we highlight the reduction of the supported M′ cations.

In model B the structure is continuous through the interface; the following simplifications can be introduced in Eqs. (7) and (8):

$$\Delta E_S^B \simeq 0; \qquad \Delta E_1^B \simeq \Delta E_2^B$$

and substituting:

$$\left(\Delta E_S^B + \Delta E_1^B - \Delta E_2^B\right) \simeq 0$$

$$r_o^B(c) \to \infty \quad \text{for each } c$$

$$\Delta E^B(c) \simeq c \cdot E_V \tag{11}$$

Only the volume energy ΔE_V (the energy required to transform a unit volume of $M'O_x$ to the structure of $M''O_y$) gives an appreciable contribution to ΔE^B and for each quantity of overlayer deposited on the support, according to model B, M′ is dispersed as much as possible on the surface.

On comparing the total energies given by the two geometries proposed we must know the explicit values of all the parameters employed; we can nonetheless note the different functional dependence of the total energies on c in the two cases:

$$\Delta E^A(c) \propto p \cdot c^{2/3} + q \cdot c$$

$$\Delta E^B(c) \propto q' \cdot c$$

A plot of the two curves is reported in Fig. 4 (assuming for simplicity $p = q' = 1$ and $q = 0.1$). For

low values of c, the surface contribution prevails and model B has a lower energy than A. We therefore hypothesize the existence of a range of c for which $\Delta E^{B}(c) < \Delta E^{A}(c)$; the value c_o for which the two plots intersect and structure A eventually becomes stable depends on all the energy parameters.

From geometrical considerations we can expect that the volume contribution becomes predominant at high values of M′ deposited on the support and, as a limiting case, for $c \rightarrow \infty$ we would expect to have two interfaced crystals, each with the structure of the pure component, as predicted by model A. Such structures might be generated by mechanically mixing of particles of discrete size of the two components; for this reason, we identify model A as a '*mechanical mixing*' structure.

The dispersion of M′ on the support at low concentrations, instead, can be obtained by chemical deposition: in this case M′, approaching the surface, finds a structure already defined and adapts to it. We have therefore labelled B as the '*chemical deposition*' model.

It is finally useful to note that the interface geometries A and B represent two limiting cases, which allow some of the energy contributions to be simplified. The real structure is probably intermediate; other structures and oxidation states can be treated using the same set of equations previously obtained. Formulating a new interface geometry and collecting all the corresponding energy parameters, allows us to plot its total energy versus that of the geometries proposed here and compare the relative stability. Eqs. (7) and (8) provide therefore a way to differentiate and rationalise the behaviour of oxide interfaces.

Let us now return to the argument of Section 2 in the light of the geometrical models just discussed. The value ΔE_V that characterizes model B represents the energy required to transform a unit volume of $M'O_x$ into $M'O_y$, with the structure proper of pure $M''O_y$, according to Eq. (10). It clearly depends on two factors: the ability of M′ to be reduced ($x > y$), and its ability to adapt to the local structure of $M''O_y$. As seen in Section 2.1, the first requirement is satisfied by all the overlayer cations. The second requirement suggests a partitioning of cations according to their preferred local environment. We create in this way two major groups: the tetrahedrally coordinated cations, comprising Si and Cr and the octahedrally coordinated, including all the others, with the exception of Zr.

That the surface structure of the support plays a major role in determining the overlayer geometry, in accord with model B, is confirmed by several experimental results: SiO_2 is less active for supporting octahedral cations than is octahedral TiO_2 [30]; at high temperatures Nb_2O_5 on SiO_2 tends to form a separate crystalline phase, rather than a Nb_2O_5/SiO_2 overlayer [36]; 'V-51 NMR' studies in V_2O_5/Al_2O_3 and V_2O_5/SiO_2 have shown that bulk-like vanadia species are present only at high vanadia loadings, that vanadia is more dispersed on Al_2O_3 than it is on SiO_2 and that on SiO_2 the amount of surface V correlates with the amount of tetrahedral V from NMR signals [37]. Furthermore, CrO_3 shows a different structure on SiO_2 than it does on Al_2O_3, TiO_2 and ZrO_2 [38], and calcination easily reduces Cr(VI) supported on Al_2O_3 to Cr(III) that gives substitutional defects in the support [39]. We note that all the above supports satisfy the chemical requirements of Section 2.1, but have different structural properties. These results confirm that CrO_3 and SiO_2 form a class of their own: to enter the octahedral group, Cr must be reduced to Cr(III), as shown by the referred work on Al_2O_3. In an analogous way, the 7 or 8-fold coordination of Zr can probably be assigned to the octahedral class; ZrO_2 shows in fact the same behaviour as TiO_2.

From the previous argument we conclude that the stoichiometry and structure of the support determine to a large extent the stoichiometry and geometry of the oxygen sublattice in the overlayer region close to the interface. The oxidation state of the supported metal cation is an important parameter that must be included in the model.

4. Conclusions

The picture of the interface presented here, although oversimplified in many respects, provides a way to link the effect of the relevant experimental (macroscopic) variables: support face exposed, overlayer face obtained, oxidation state and local coordination number of the overlayer cation, overlayer loading. It therefore represents a useful guideline to solve important experimental problems: the influence of the support on the overlayer reducibility; which face of the support is more likely to give maximum interaction with the overlayer; which phase and face of the overlayer is interacting most strongly with a given support structure and the effect of the overlayer loading on the above properties. By imposing one or more of the above variables in the model, we can determine which combination of the others is more likely to yield the desired result, thus having an effective way of *tailoring* the properties of the exposed surface sites. Our approach has therefore the capacity to be *predictive*.

We should like to emphasize that the general model discussed in Section 3 is formulated in such a way that the energy parameters can be quantified in a natural way using computer modelling techniques, of the kind employed in Ref. [34,35]. Computer modelling provides in fact the appropriate link between a specified geometry and its physical representation and provides a direct way to compare selected geometrical configurations of the interface. In this contribution attention has been drawn to the presentation and discussion of the model; a detailed description of the application to WO_3/TiO_2 will be presented elsewhere [40,41]. A few general conclusions can nonetheless be pointed out:

At low loadings, c, the effect of the support is maximised and determines to a large extent the stoichiometry and geometry of the oxygen sublattice in the overlayer.

The arguments presented in Section 3, both from the model and the experimental view, suggest that the *chemical deposition* geometry of model B can be adopted by the overlayer. In this situation, the cation M′ is reduced and still retains good Lewis-acid properties (all the supports are good Lewis acids). Assuming that Eq. (10) is reversible (the capacity of exchanging oxygen between overlayer and gas phase has been reported [42]), M′ is also able to increase its coordination; it then provides a suitable centre on which Eqs. (1) and (2) can both take place.

By improving the region of stability of the interface geometry of model B, we can transform the catalytic activation of a solid via substitution of the dopants *in* the support to a catalytic activation via substitution *on* the support.

Having a means to estimate c_o appears to be particularly important: in a neighbourhood of c_o, in fact, the stability of the two oxidation states of the overlayer cation is comparable and the influence of admolecules on the relative stability is therefore maximised. This situation appears to be particularly promising to obtain efficient catalysts for reactions involving redox steps.

Acknowledgements

Financial support for this work from ICI Katalco and Molecular Simulations Inc. is gratefully acknowledged.

References

[1] H. Bosch and F. Janssen, Catal. Today 2 (1988) 369.
[2] G.C. Bond and S.F. Tahir, Appl. Catal. 71 (1991) 1.

[3] T. Yamaguchi, Y. Tanaka and K. Tanabe, J. Catal. 65 (1980) 442.
[4] M. Imanari and Y. Watanabe, in: T. Seiyama and K. Tanabe (Eds.), New Horizons in Catalysis, Proc. 7th Int. Congr. Catal., Tokyo, 1980, Elsevier, Amsterdam, 1980, p. 841.
[5] S. Morikawa, K. Takahashi, J. Mogi and S. Kurita, Bull. Chem. Soc. Jpn. 55 (1982) 2254.
[6] S.S. Chan, I.E. Wachs, L.L. Murrell, L. Wang and W.K. Hall, J. Phys. Chem. 88 (1984) 5831.
[7] D.C. Vermaire and P.C. van Berge, J. Catal. 116 (1989) 309.
[8] L.J. Pinoy and L.H. Hosten, Catal. Today 17 (1993)151.
[9] L. Lietti, J. Svachula, P. Forzatti, G. Busca, G. Ramis and F. Bregani, Catal. Today 17 (1993) 131.
[10] B.L. Duffy, H.E. Curry-Hyde, N.W. Cant and P.F. Nelson, Preprints, Symposium on NO_x reduction, ACS, Division of Petroleum Chemistry, San Diego, CA, March 1994, p. 125.
[11] K.A. Vikulov, A. Andreini, E.K. Poels and A. Bliek, Catal. Lett. 25 (1994) 49.
[12] G. Centi, C. Nigro, S. Perathoner and G. Stella, Catal. Today 17 (1993) 159.
[13] H.R. Matralis, C. Papadopoulous, C. Kordulis, A.A. Elguezabal and V.C. Corberan, Appl. Catal. A 126 (1995) 365.
[14] J. Lebars, J.C. Vedrine, A. Auroux, S. Trautmann and M. Baerns, Appl. Catal. A 88 (1992) 179.
[15] M. Derewinski, J. Haber, R. Kozlowski, W.A. Zazhigalov, J.P. Zajcev, I.W. Bacherikowa and W.M. Belousov, Bull. Pol. Acad. Sci. Chem. 39 (1991) 403.
[16] M. Wojciechowska and S. Lomnicki, Catal. Lett. 33 (1995) 217.
[17] M. Wojciechowska, S. Lomnicki and W. Gut, Pol. J. Chem. 69 (1995) 939.
[18] J. Haber, M. Wojciechowska and W. Gut, Bull. Pol. Acad. Sci. Chem. 39 (1991) 383.
[19] J.M. Jehng, I.E. Wachs, B.M. Weckhuysen and R.A. Schoonheydt, J. Chem. Soc. Faraday Trans. 91 (1995) 953.
[20] B.M. Reddy, ACS Symp. Series, Vol. 523 (1993) p. 204.
[21] D.S. Kim, J.M. Tatibonet and I.E. Wachs, J. Catal. 136 (1992) 209.
[22] U.S. Ozkan, Y. Cai and M.W. Kumthekar, Appl. Catal. A 96 (1993) 365; U.S. Ozkan, Y. Cai, M.W. Kumthekar and L. Zhang, J. Catal. 142 (1993) 182.
[23] S. Scrinivasan and A.K. Datye, Catal. Lett. 15 (1992) 155.
[24] A. Burrows, R.W. Devenish, R.W. Joyner, C.J. Kiely, H. Knozinger and F. Lange, Inst. Phys. Conf. Series, Vol. 138 (1993) p. 481; A. Burrows, C.J. Kiely, R.W. Joyner, H. Knozinger and F. Lange, Catal. Lett., 39 (1996) 219.
[25] F. Roozeboom, T. Fransen, P. Mars and P.J. Gellings, Z. Anorg. Allg. Chem. 449 (1979) 25.
[26] M. del Arco, M.J. Holgado, C. Martin and V. Rives, Langmuir 6 (1990) 801.
[27] J.P. Chen and R.T. Yang, Appl. Catal. A 80 (1992) 135.
[28] L.J. Alemany, L. Lietti, N. Ferlazzo, P. Forzatti, G. Busca, E. Giamello and F. Bregani, J. Catal. 155 (1995) 117.
[29] J. Nickl, Ch. Schild, A. Baiker, M. Hund and A. Wokaun, Fresenius J. Anal. Chem. 346 (1993) 79.
[30] J. Nickl, D. Dutoit, A. Baiker, U. Scharf and A. Wokaun, Ber. Bunsenges. Phys. Chem. 97 (1993) 217.
[31] M. Galanfereres, R. Mariscal, L.J. Alemany, J.L.G. Fierro and J.A. Anderson, J. Chem. Soc. Faraday Trans. 90 (1994) 3711.
[32] J.A. Odriozola, H. Heinemann, G.A. Somorjai, F.G. Garcia de la Banda and P. Pereira, J. Catal. 119 (1989) 71.
[33] R.W.G. Wyckoff, Crystal Structures, 2nd Ed., Interscience, New York, 1965.
[34] D.C. Sayle, A.R. George, C.R.A. Catlow, M.A. Perrin and P. Nortier, Rev. Inst. Fr. Pet. 51 (1996) 43; D.C. Sayle, C.R.A. Catlow, M.A. Perrin and P. Nortier, J. Phys. Chem., 100 (1996) 8940.
[35] C.A. Scamehorn, N.M. Harrison and M.I. McCarthy, J. Chem. Phys. 101 (1994) 1547.
[36] S. Denofre, Y. Gushikem, S.C. Decastro and Y. Kawano, J. Chem. Soc. Faraday Trans. 89 (1993) 1057.
[37] M.M. Koranne, J.G. Goodwin and G. Marcelin, J. Catal. 148 (1994) 369.
[38] M.A. Vuurman, I.E. Wachs, D.J. Stufkens and A. Oskam, J. Mol. Catal. 80 (1993) 209.
[39] A. Rahman, M.H. Mohamed, M. Ahmed and A.M. Aitani, Appl. Catal. A 121 (1995) 203; B.M. Weckhuysen, L.M. Deridder, P.J. Grobet and R.A. Schoonheydt, J. Phys. Chem. 99 (1995) 320.
[40] F. Corà, A. Patel, N.M. Harrison, R. Dovesi and C.R.A. Catlow, J. Am. Chem. Soc., 118 (1996) 12174; F. Corà, Master Thesis, University of Portsmouth, Portsmouth, UK (1995).
[41] F. Corà and C.R.A. Catlow, in preparation.
[42] U.S. Ozkan, Y. Cai and M.W. Kumthekar, Preprints, Symposium on NO_x reduction, ACS, Division of Petroleum Chemistry, San Diego, CA, March 1994, p. 121.